Taylor & Francis
Taylor & Francis Group

Artificial Cells, Nanomedicine, and Biotechnology

An International Journal

ISSN: (Print) (Online) Journal homepage: https://www.tandfonline.com/loi/ianb20

Pectin-conjugated magnetic graphene oxide nanohybrid as a novel drug carrier for paclitaxel delivery

Nizamudin Awel Hussien, Nuran Işıklan & Mustafa Türk

To cite this article: Nizamudin Awel Hussien, Nuran Işıklan & Mustafa Türk (2018) Pectin-conjugated magnetic graphene oxide nanohybrid as a novel drug carrier for paclitaxel delivery, Artificial Cells, Nanomedicine, and Biotechnology, 46:sup1, 264-273, DOI: 10.1080/21691401.2017.1421211

To link to this article: https://doi.org/10.1080/21691401.2017.1421211

ARTIFICIAL CELLS, NANOMEDICINE, AND BIOTECHNOLOGY
2018, VOL. 46, NO. S1, S264–S273
https://doi.org/10.1080/21691401.2017.1421211

Pectin-conjugated magnetic graphene oxide nanohybrid as a novel drug carrier for paclitaxel delivery

Nizamudin Awel Hussien[a], Nuran Işıklan[a] and Mustafa Türk[b]

[a]Department of Chemistry, Kırıkkale University, Kırıkkale, Turkey; [b]Department of Bioengineering, Kırıkkale University, Kırıkkale, Turkey

ABSTRACT

Recent studies have shown that graphene oxide (GO) drug carrier functionalized with biocompatible natural polymers lead to higher loading efficacy and better stability with diminished cellular toxicity. Pectin (PEC) is one of the polysaccharide natural polymers, which has the potential to be used for drug delivery. In this work, we have successfully developed a novel PEC-conjugated magnetic GO nanocarrier for effective delivery of paclitaxel. The structure, surface morphology and thermal stability of the nanohybrid were investigated using Fourier transform infrared spectroscopy (FTIR), X-ray diffraction (XRD), transmission electron microscopy (TEM) and zeta-sizer. Moreover, drug loading and release performance were studied by UV–vis absorption spectra. The cytotoxicity test was also performed by MTT test using L-929 fibroblast normal cell and MCF-7 cancer lines. The prepared nanocarrier showed an improved stability with enhanced drug loading capacity. Additionally, pH-responsive release analysis of the nanohybrid illustrated higher drug release at endosomal pH of cancer cell than that of normal physiological environment. Besides, cytotoxicity test demonstrated the synthesized nanohybrid is biocompatible, having very high relative cell viability. Bearing in mind these findings, the designed multifunctional nanohybrid drug carrier will be a good candidate for cancer drug delivery.

ARTICLE HISTORY
Received 29 September 2017
Revised 18 December 2017
Accepted 20 December 2017

KEYWORDS
Nanocarrier; graphene oxide; polymer; pectin; biocompatibility; drug delivery

Introduction

Chemotherapy is the main cancer therapeutic method, which has been used for most of cancer diseases. Nevertheless, the inefficiency due to drug resistance and side effects, such as hair loss, nausea, toxicity to cardiac, liver damage, etc. has limited its application on cancer treatment [1,2]. Hence, several studies have been ongoing to design an efficient drug delivering mechanism that can improve cellular uptake and decrease side effects. Recent studies demonstrated that nanomaterial based drug carriers are the most potential drug delivering agents due to their higher loading capacity (LC), efficient release and targeted delivery [3].

Graphene oxide (GO) based nanocarriers have been emerging as a novel and viable drug carrier for controlled drug delivery systems [4–6]. GO is an oxidized form of graphene containing numerous oxygen holding functional groups, such as carboxyl, hydroxyl and epoxy on its layer, which enhance drug LC, water-solubility and provides a basis for further functionalization of GO to other materials [7,8]. Lately, GO functionalized with iron oxide (Fe_3O_4) has gained more attention owing to its advantageous magnetic properties to be applied in targeting tumour cells [9]. Magnetic nanomaterials are guided by external magnetic field to carry drugs into cancer cell, improving therapeutic efficiency and decreasing the side effects [10]. Although, GO and its derivative nanocarriers, including magnetic GO, are accepted as promising materials because of their exceptional physiochemical properties; their poor dispersity in electrolyte solutions, agglomeration in aqueous solutions and low colloidal stability limited their application in cancer therapy [5,6]. Recently, modification of GO based nanocarriers with biomaterials, such as natural polymers, was found to be one of the best way to encounter these challenges.

Current studies indicated that polymer functionalized GO based drug carriers have been playing an important roles in systematic drug delivery since functionalization improves their biocompatibility, drug loading and release performance [11,12]. Moreover, modification of GO with polymers is found to be the most effective way to decrease agglomeration, so that prevents instability and improves efficiency [13]. Functionalization of GO with polymers was first reported by Liu et al., who successfully modified GO by PEG to deliver SN38 [14]. Subsequently, several related studies have been reported. For instance, a gelatin conjugated graphene sheet was synthesized by An et al. for effective delivery of methotrexate [15]. Mianehrow et al. investigated stabilization of GO with hydroxyethyl cellulose to increase the stability of GO in saline environments [16]. Lei et al. have prepared chitosan/sodium alginate functionalized GO, having improved stability, aqueous solubility and drug LC [12]. Until now, functionalization of GO is one of the latest research area in the biomedical application of graphene and its derivatives.

In the current paper, for the first time we reported pectin (PEC) conjugated magnetic GO nanomaterial for efficient

CONTACT Nuran Işıklan nuranisiklan@hotmail.com Department of Chemistry, Faculty of Arts and Sciences, Kırıkkale University, 71450 Yahşihan, Kırıkkale, Turkey

delivery of paclitaxel (PAC). PEC is one of the natural polymers that has been employed in the delivery of drugs [17–19]. PEC has important properties, such as; easily adjustable, higher content of water and capability to restrain cells, drugs and genes, that makes it suitable for biomedical applications [20–22]. Moreover, it is an effective reductant in the synthesis of biological materials [18,23]. However, there is no report indicating the use of PEC to functionalize magnetic GO to improve drug loading and release performance, biocompatibility and stability of the hybrid nanocarrier, so that to obtain an efficient drug delivery vehicle. In this study, Fe_3O_4 nanoparticle was attached on the layer of GO to synthesize magnetic nanocarrier and reduce cytotoxicity. Then, PEC was conjugated as stabilizing agent to enhance biocompatibility, avoid aggregation and increase stability. Finally, PAC, anticancer drug, was loaded. After preparation of the nanomaterial, the physicochemical properties were characterized. Drug loading and release performance were investigated. Moreover, the cytotoxicity effect of the nanomaterial was studied using L-929 fibroblast normal cell and MCF-7 cancer cell.

Experimental

Materials and methods

GO powder was purchased from Graphene Supermarket (Graphene Laboratories Inc., Calverton, NY). Pectin, esterified potassium salt from citrus fruit (55–70%) was obtained from Sigma-Aldrich (Bratislava, Slovakia). Triethylene glycol (TREG $\geq$ 99%) was purchased from Merck Millipore (Darmstadt, Germany). Iron(III)acetylacetonate ($Fe(acac)_3 \geq 99.9\%$) and PAC ($\geq$97%) were delivered by Sigma-Aldrich (St. Louis, MO). The rest of the chemicals used were analytical grade.

Characterization

Surface morphology was investigated by transmission electron microscopy (TEM-3010, Jeol, Tokyo, Japan). Thermal characteristic was assessed using thermogravimetric analysis (TGA, Q500, TA Instruments Inc., Milford, MA). The optical properties were determined by Ultra Violet (UV–Vis) Spectrophotometer (Lambda 35, PerkinElmer, San Diego, CA). Fourier transform infrared spectroscopy (FTIR) spectra were recorded by FTIR Spectrophotometer, Vertex 70v, Bruker (Billerica, MA). X-ray diffractometer (Ultima IV, Rigaku, Tokyo, Japan) was used to investigate X-ray diffraction (XRD) pattern. Particle size and zeta potential were examined via Zetasizer (Nano ZS 90, Malvern Instruments Ltd., Malvern, UK). The samples were prepared using deionized water having concentration of 0.1 mg mL^{-1}. The ratio of Fe_3O_4 particles loaded on the GO layer was measured by inductively coupled plasma optical emission spectrometry (ICP-OES, Spectro blue, Kleve, Germany). The magnetic property of the nanocarriers was assessed by Physical Properties Measurement System (PPMS) (Cryogenic Limited PPMS, London, UK), at room temperature with applied magnetic field ranging between −2000 and +2000 Oe.

Preparation of GO-Fe_3O_4 magnetic nanocarrier

GO-Fe_3O_4 magnetic nanocarrier was prepared by conjugating Fe_3O_4 nanoparticle on the surface of GO. Briefly, 40 mg of GO powder was dispersed in 50 mL of TREG and sonicated for 5 h to breakdown the GO nanomaterial to minimum size. Forty milligrams of $Fe(acac)_3$ was added into the GO solution along with 45-min further sonication. Then, the solution was gradually heated to 278 °C for 1 h under argon gas atmosphere and waited for 50-min at 278 °C. After it was cooled, the produced GO-Fe_3O_4 hybrid was collected magnetically and washed four times using ethanol and deionized water. Lastly, the synthesized nanomaterial was dried at 60 °C.

Conjugation of PEC with GO-Fe_3O_4

Pectin conjugation to GO-Fe_3O_4 was performed by simple mixing mechanism. First, 3 mL of PEC (0.5 mg mL^{-1}, deionized water) was mixed with 4 mL of GO-Fe_3O_4 (1 mg mL^{-1}, 7.4 PBS) in a 20-mL tube. Next, the solution was vortexed for 5-min and stirred for 24 h. The PEC functionalized nanocarrier (PEC-GO-Fe_3O_4) was separated using magnet. Finally, the prepared nanocarrier was dried, after washing by deionized water three times.

Drug loading and in vitro release

To load PAC on the nanocarrier, 1 mL of 0.5 mg mL^{-1} of PAC was added on 2 mL, 1 mg mL^{-1} of PEC-GO-Fe_3O_4 solution and mixed for 24 h, stirring at 25 °C. The PAC loaded nanocarrier was collected using magnet and washed three times before drying. Finally, the prepared PEC-GO-Fe_3O_4-PAC nanocomplex was kept at 8 °C. Drug LC and entrapment efficiency (EE%) were calculated by using Equations (1) and (2).

$$LC\% = \frac{\text{mass of PAC in the nanocarrier}}{\text{mass of nanocarrier}} \times 100 \quad (1)$$

$$EE\% = \frac{\text{mass of PAC in the nanocarrier}}{\text{mass of PAC initially loaded}} \times 100 \quad (2)$$

Schematic illustration of the synthesis of GO-Fe_3O_4, PEC-GO-Fe_3O_4 and PEC-GO-Fe_3O_4-PAC is presented in Scheme 1.

In vitro drug release was examined at different pH solutions; such as, 5.5 and 7.4. Briefly, 1 mg of PEC-GO-Fe_3O_4-PAC was dispersed by 5 mL of buffer solution, in a test tube of 20 mL. The test tube was placed in a water bath of 37 °C, stirring at 100 rpm. At certain time intervals (1, 2, 3, 4, 5, 6, 24, 48, 72, 96 and 120 h), 500 µL supernatant was collected and replaced by equal amount of fresh buffer solution. The amount of the PAC released at each time interval was determined by the help of UV–vis absorption spectra of the collected supernatant at 229 nm. All tests were done three times and standard deviation (SD) of each test was calculated.

Cytotoxicity assay

In vitro cytotoxicity of the nanocarrier was studied using L-929 fibroblast normal cell and MCF-7 cancer cell, following 3-(4,5-dimethylthiazol-2-yl)-2,5-diphenyltetrazolium bromide (MTT) assay [24]. After sample treatment, the L-929 fibroblast

normal cell and MCF-7 cancer cell were incubated for 24 h and 72 h, respectively. ELISA micro-plate reader was used to measure the optical density of the treated cells. The relative cell viability was evaluated by Equation (3) [25].

$$\text{Relative cell viability } (\%) = \frac{\text{average optical density of the sample}}{\text{average optical density of control}} \times 100 \quad (3)$$

Statistical analysis

The statistical calculations were carried out via Student's *t*-test and one-way ANOVA using SPSS 16.0 software (IBM, Armonk, NY). The data were considered statistically different when the level of significance (p) $< .05$. The results were given as mean ± SD. For all experiments, at least three independent measurements were done.

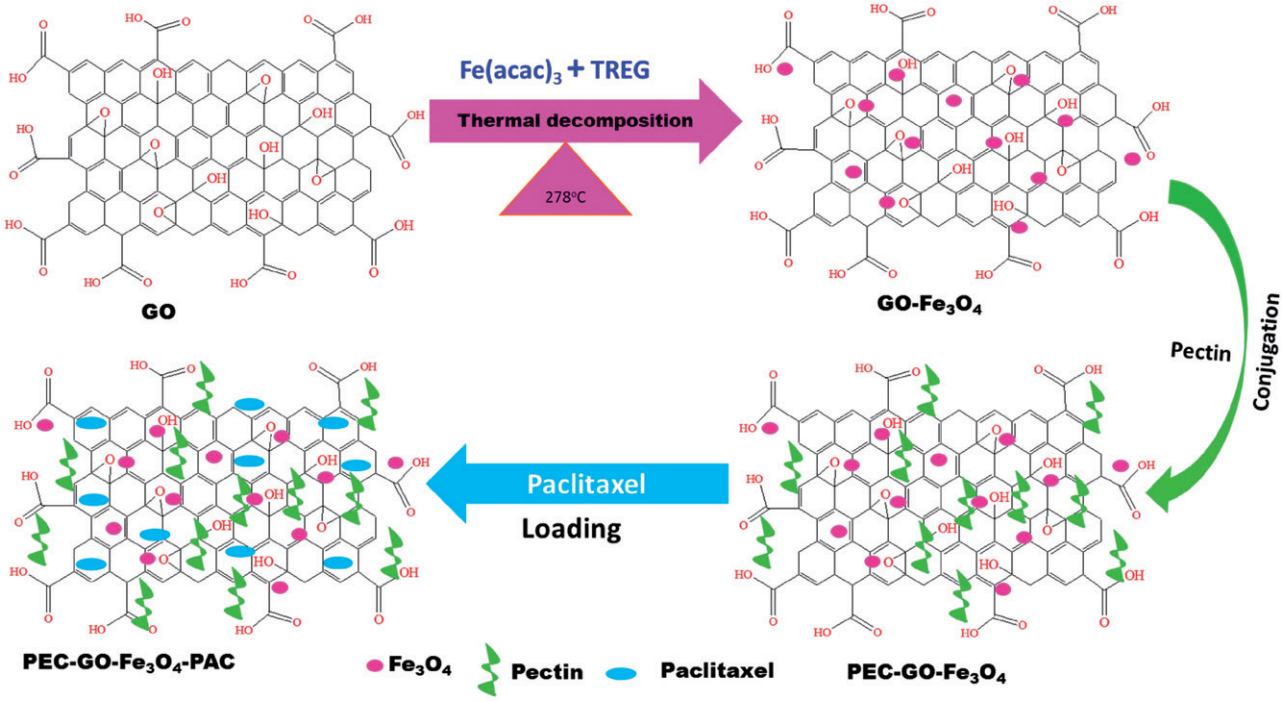

Scheme 1. Schematic illustration of the synthesis of GO-Fe_3O_4, PEC-GO-Fe_3O_4 and PEC-GO-Fe_3O_4-PAC.

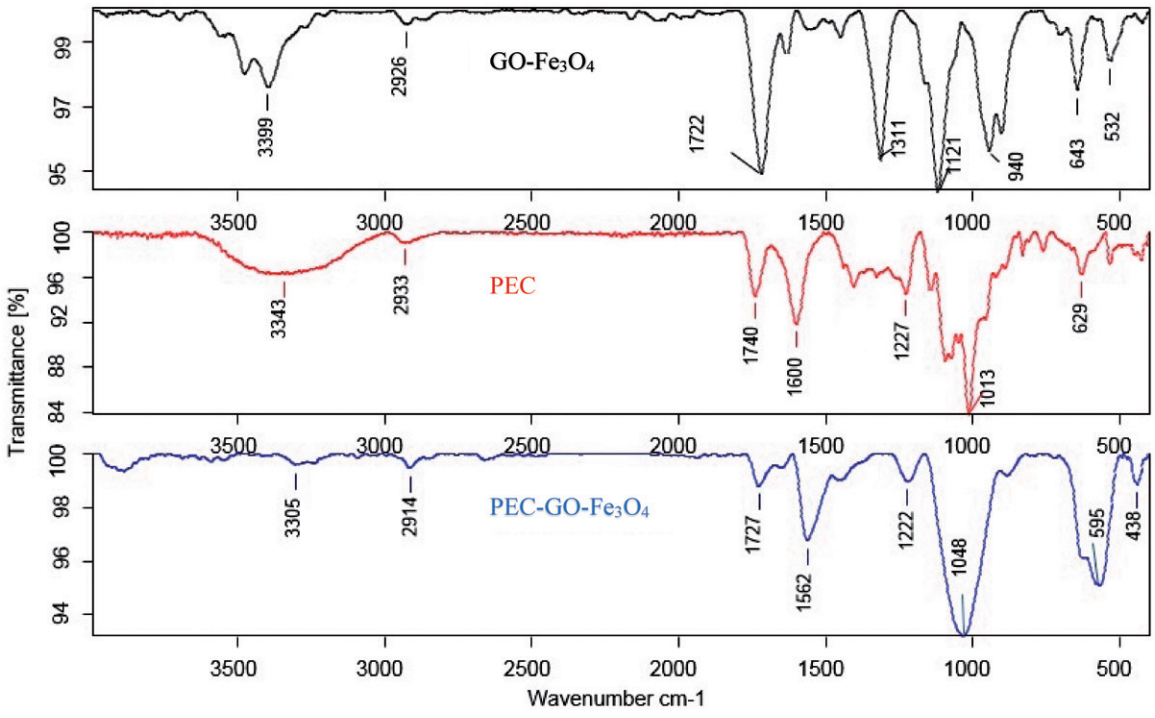

Figure 1. FTIR spectra of GO-Fe_3O_4, PEC and PEC-GO-Fe_3O_4.

Result and discussions

Characterization of PEC-GO-Fe_3O_4

FTIR spectrum of the GO-Fe_3O_4, PEC and PEC-GO-Fe_3O_4 is shown in Figure 1. FTIR spectrum of GO-Fe_3O_4 illustrated peaks at 3399 cm^{-1} (O–H stretching), 1722 cm^{-1} (C=O asymmetric stretching), 1311 cm^{-1} (C–H bending), 1121 and 940 cm^{-1} (C–O stretching of epoxy and hydroxy). Moreover, the two peaks found at 643 cm^{-1} and 532 cm^{-1} were corresponding to Fe–O bond interactions [26,27]. In the spectrum of PEC, the peaks at 3343 cm^{-1} and 2933 cm^{-1} represented O–H and C–H bond stretching. The peak at 1740 cm^{-1} is the characteristic peak of PEC, which corresponds to vibrational stretching of esterified carbonyl group. The peaks at 1600 cm^{-1}, 1227 cm^{-1} and 1013 cm^{-1} corresponded to C=O of carboxylic acid, C–O bond of an ester group and C–O–C bond vibrational stretching, respectively. The spectrum of PEC-GO-Fe_3O_4 illustrated most of the characteristic peaks of both GO-Fe_3O_4 and PEC with slight shifts in some cases. The peak at 3305 cm^{-1} corresponded to O–H stretching, however, the peak strength is weak because of reduction characteristics of PEC [18]. The peaks at 1727 cm^{-1} and 1562 cm^{-1} are related to C=O bond stretching of ester and carboxylic groups. Moreover, the peaks at 1222 cm^{-1} and 1048 cm^{-1} could be assigned to C–O bond of an ester group originated from PEC and C–O–C bond stretching of the GO-Fe_3O_4. The results verify the conjugation of PEC on the magnetic GO-Fe_3O_4 layer.

The XRD pattern of GO, GO-Fe_3O_4 and PEC-GO-Fe_3O_4 is presented in Figure 2. The XRD pattern of GO depicted characteristic diffraction peaks at 2θ values of 10.68°, which originated from (001) reflection of GO and a broad peak at 2θ values of 22°, that is associated to the diffraction of layer of graphene sheet. However, GO-Fe_3O_4 and PEC-GO-Fe_3O_4 illustrated diffraction peaks at 2θ values of 24.22°, 30.24°, 35.67°, 43.56°, 57.44° and 63.12°. The peak at 2θ values of 24.22° is related to the diffraction of main graphene sheet [28,29]. The rest of the peaks corresponded to (220), (311), (400), (511) and (440) planes of cubic structure of the Fe_3O_4 [30], indicating Fe_3O_4 nanoparticles are loaded successfully on the layer of GO. The peak characteristics for citrus PEC were not clearly observed. The reason could be enclosed by GO-Fe_3O_4 peaks, or absent due to low concentration (lower than XRD detection limits) of the conjugated PEC. Similar results were obtained by Kadam et al. [31].

Surface morphology and particle size of GO-Fe_3O_4 and PEC-GO-Fe_3O_4

The surface morphology of GO, GO-Fe_3O_4 and PEC-GO-Fe_3O_4 nanocarriers was studied using TEM. TEM images of GO (Figure 3(a)) showed that the surface was smooth all-round

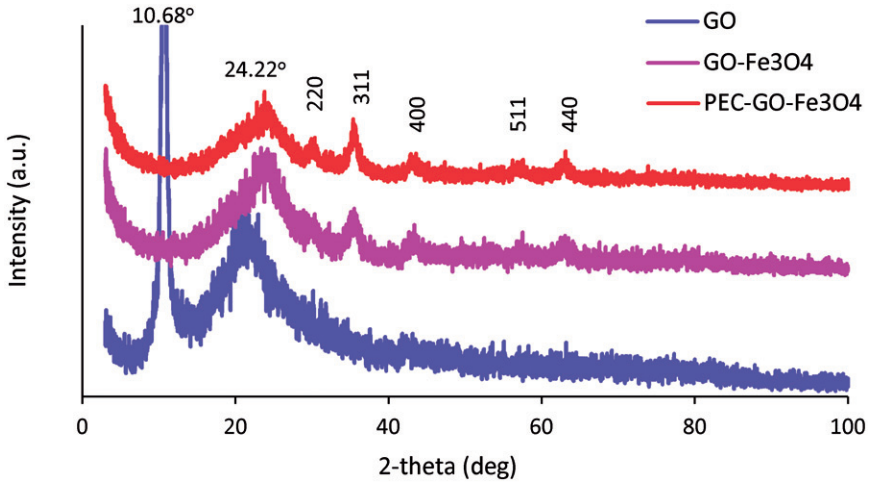

Figure 2. XRD spectrum of GO, GO-Fe_3O_4 and PEC-GO-Fe_3O_4.

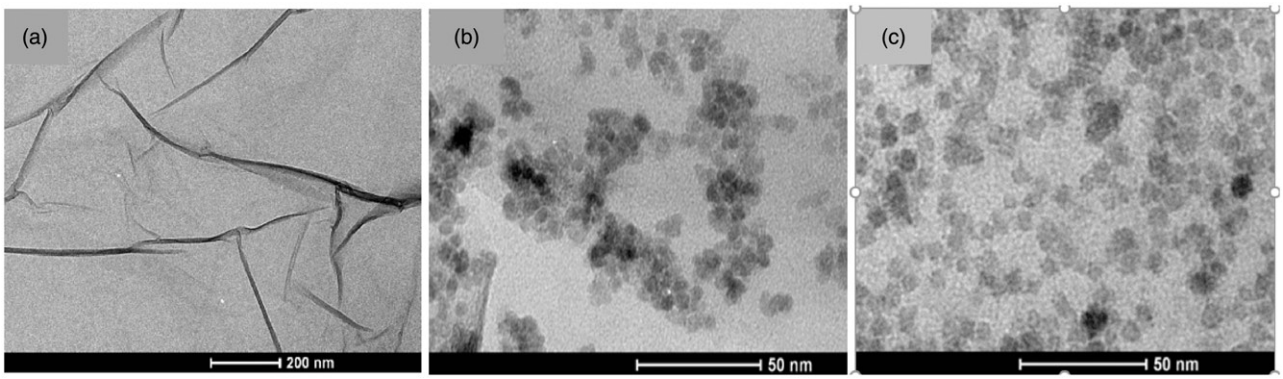

Figure 3. TEM images of GO (a), GO-Fe_3O_4 (b) and PEC-GO-Fe_3O_4 (c).

the layer. But, the surface of GO-Fe_3O_4 (Figure 3(b)) was found to be decorated by Fe_3O_4 nanoparticles distributed on the layer. The size of the Fe_3O_4 is estimated to be between 6 and 12 nm. The surface of PEC-GO-Fe_3O_4 (Figure 3(c)) was observed relatively blurred, containing a bit larger Fe_3O_4 throughout. Moreover, the thickness of the layer is estimated to be increased due to the conjugated PEC covering the surface of GO-Fe_3O_4. The effect of PEC conjugation on the surface charge was also investigated using Zetasizer. The result showed the conjugation significantly altered the surface charge of the nanocarrier. The zeta potential of GO-Fe_3O_4 was −20.17 mV, but after PEC conjugation it increased to −26.03 mV, improving the colloidal stability of the nanocarrier. On the other hand, particle size analysis of GO-Fe_3O_4, PEC-GO-Fe_3O_4 and PEC-GO-Fe_3O_4-PAC was performed. Table 1 presents the average particle size and polydispersity index of GO-Fe_3O_4, PEC-GO-Fe_3O_4 and PEC-GO-Fe_3O_4-PAC. As it can be seen from the table, the average sizes of GO-Fe_3O_4, PEC-GO-Fe_3O_4 and PEC-GO-Fe_3O_4-PAC nanocarriers are 509 ± 55 nm, 534 ± 42 nm and 533 ± 55 nm, respectively. The data showed a bit enlargement in the particle size of GO-Fe_3O_4 as PEC conjugation. This increment may be explained by the conjugation of some of PEC chains with the carboxylic groups of GO at the edge of the sheet. Furthermore, to evaluate the extent of GO modification by the attachment of Fe_3O_4 and PEC, the ratio of each components was calculated. The calculation was performed by using TGA thermogram and ICP-OES spectrometry. The result was found to be 15.17%, 15.36% and 69.47%, respectively, for Fe_3O_4, PEC and GO, indicating about 31% modification of the main GO nanomaterial by the conjugation of Fe_3O_4 and PEC.

Table 1. The average particle size and polydispersity index of GO-Fe_3O_4, GO-Fe_3O_4-PEC, GO-Fe_3O_4-PEC-PAC.

Nanocarriers	Size (nm)	PDI
GO-Fe_3O_4	509.00 ± 55.57	0.526 ± 0.28
PEC-GO-Fe_3O_4	534.47 ± 41.95	0.545 ± 0.12
PEC-GO-Fe_3O_4-PAC	532.90 ± 54.62	0.588± 0.09

Results are given as the mean ± SD of $n = 3$.

Magnetic properties of PEC-GO-Fe_3O_4 and PEC-GO-Fe_3O_4-PAC

The magnetic properties of PEC-GO-Fe_3O_4 and PEC-GO-Fe_3O_4-PAC were analysed at room temperature by PPMS. As illustrated in Figure 4, the maximum saturation magnetization of the PEC-GO-Fe_3O_4 and PEC-GO-Fe_3O_4-PAC was recorded as 9.04 and 7.67 $emug^{-1}$, at the given magnetic field range. There was ∼1.4 $emug^{-1}$ difference between the saturation magnetization of the PEC-GO-Fe_3O_4 and PEC-GO-Fe_3O_4-PAC due to PAC loading. The PAC covers the Fe_3O_4 particles reducing their response to the external magnetic field [32]. Besides, loading of PAC alters the ratio of the components in the PEC-GO-Fe_3O_4-PAC, particularly, Fe_3O_4 particles that are responsible for the magnetic character. On the other hand, the hysteresis loops of both nanocarriers revealed an S-like curve having zero remanence and coercivity, indicating the superparamagnetic characteristics of the nanocarriers [33].

Thermal characteristics of PEC and PEC-GO-Fe_3O_4

Thermal characteristics of PEC and PEC-GO-Fe_3O_4 were studied using TGA. Figure 5 presents the TGA thermograms of PEC and PEC-GO-Fe_3O_4. The TGA measurement showed three regions of weight loss for pure PEC (Figure 5(a)). The first weight loss (8.9%) was observed at temperature less than 145 °C, which is due to the evaporation of solvent molecules. The second region, which was between 145 °C and 370 °C, was associated to the breakdown of oxygen containing groups. The last region of weight loss (370–900 °C) is related to the oxidation of carbon molecules. When the temperature reached 900 °C, 95% of the sample's weight was lost. The TGA thermogram of PEC-GO-Fe_3O_4 (Figure 5(b)) illustrated only 10.8% weight loss until 750 °C, indicating significant thermal stability increment due to PEC conjugation. The second weight loss, which was observed between 750 °C and 900 °C, is associated to the decomposition of the carbon molecules.

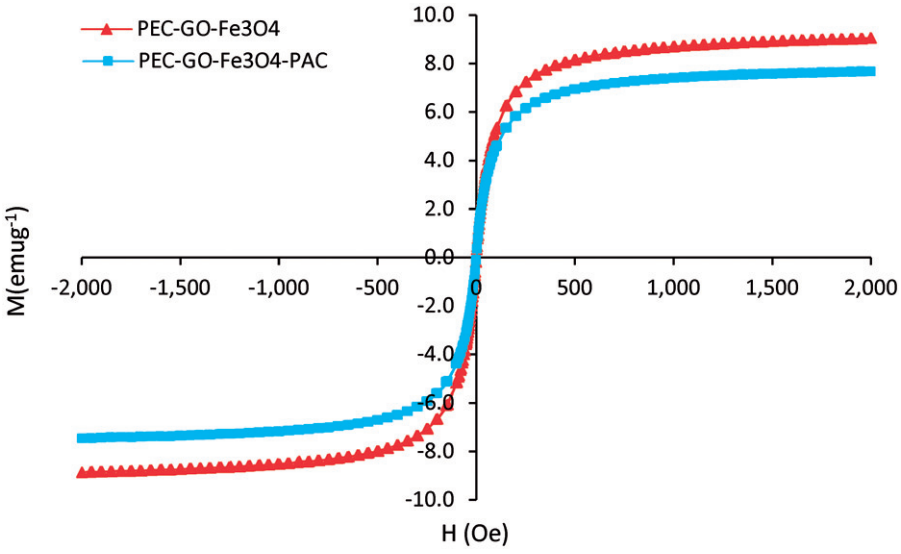

Figure 4. The magnetization hysteresis loop of PEC-GO-Fe_3O_4 and PEC-GO-Fe_3O_4-PAC at room temperature, between −2000 and +2000 Oe.

Drug loading

Drug loading performance of GO-Fe_3O_4 and PEC-GO-Fe_3O_4 was examined using PAC as a cancer drug. GO-Fe_3O_4 and PEC-GO-Fe_3O_4 consist of hydrophobic carbons and aromatic groups. There are also oxygen containing groups (such as, –OH and –COOH), which make the nanocarriers amphiphilic in nature [34]. The loading of PAC onto GO-Fe_3O_4 and PEC-GO-Fe_3O_4 nanocarriers was due to hydrophobic interactions and π–π stackings between these hydrophobic and aromatic groups of the nanocarriers and the PAC [35]. The π–π stacking is triggered by intermolecular overlap between p-orbitals of the aromatic groups of the nanocarrier and the drug [36]. Moreover, the presence of active functional groups (–OH and –COOH) in the nanocarrier could facilitate interactions with the –OH, –C=O and –NH of PAC, forming hydrogen bonding [37]. Loading capacity and EE% were determined by UV–vis absorption peak of PAC at 229 nm. The LC% and EE% of GO-Fe_3O_4 and PEC-GO-Fe_3O_4 are illustrated in Figure 6. The EE% were found to be 78.28 ± 5.25 and 84.83 ± 5.33 for GO-Fe_3O_4 and PEC-GO-Fe_3O_4, respectively. Similarly, the LC% was recorded as 33.35 ± 3.10 and 36 ± 3.21 for GO-Fe_3O_4 and PEC-GO-Fe_3O_4. Therefore, PEC conjugation enhanced the loading performance of GO-Fe_3O_4. This increment may be due to the conjugation of PEC increased the surface area of the nanocarrier to load more drugs, assuming that part of PEC functional groups conjugated to the edge of the nanocomposite. Moreover, there could be a possibility of hydrogen bonding interaction between active functional groups on the PEC structure and the drug, which may be the cause for the observed drug loading performance enhancement [16].

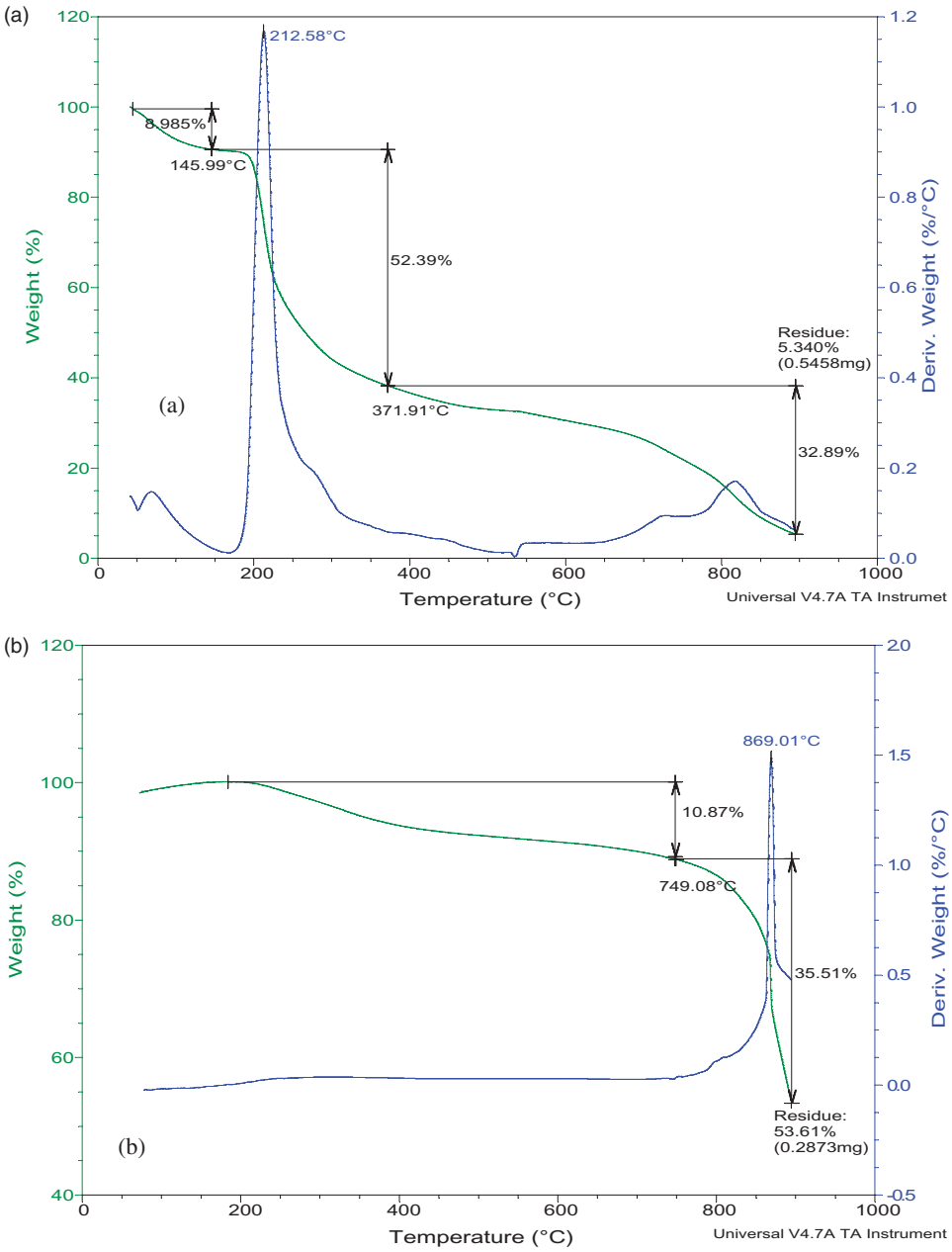

Figure 5. TGA thermogram of PEC (a) and PEC-GO-Fe_3O_4 (b).

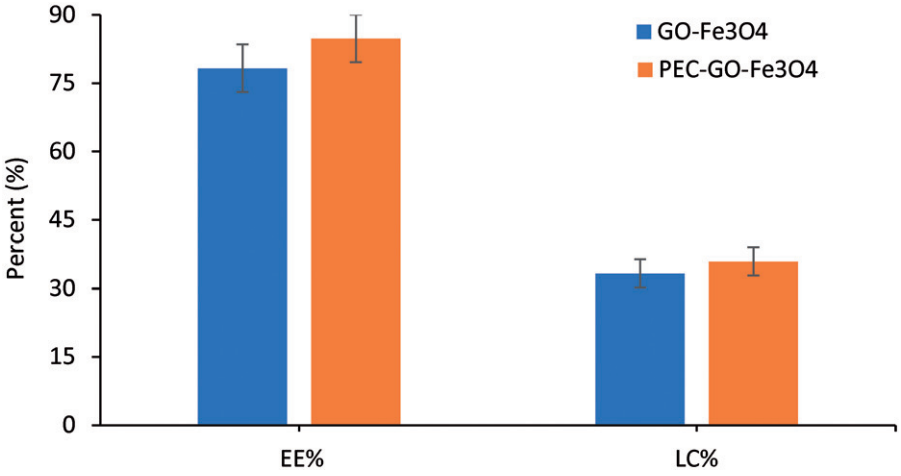

Figure 6. The LC% and EE% of GO-Fe_3O_4 and PEC-GO-Fe_3O_4. Data were given as mean ± SD ($n = 3$).

pH-sensitive drug release

In vitro drug release ability of GO-Fe_3O_4 and PEC-GO-Fe_3O_4 was investigated to assess the effect of PEC conjugation on the release efficiency of GO-Fe_3O_4 nanocarrier. The release was studied at pH 5.5 and 7.4, representing endosomal pH of cancer cell and normal physiological environment, respectively. Figure 7(a,b) presents cumulative release of PAC from GO-Fe_3O_4-PAC and PEC-GO-Fe_3O_4-PAC at pH 5.5 and 7.4 mediums. GO-Fe_3O_4-PAC and PEC-GO-Fe_3O_4-PAC released 17.89 ± 1.12% and 22.55 ± 1.99% at pH 7.4, respectively. Besides, 23.72 ± 1.75% and 30.65 ± 2.06% were released by GO-Fe_3O_4-PAC and PEC-GO-Fe_3O_4-PAC at pH 5.5, respectively. As it can be seen from the release profile, PEC conjugated nanocarrier illustrated enhancement in the release performance at both pH mediums. This increment was statistically significant ($p < .05$). The modification in the morphology and charge of the surface of GO-Fe_3O_4, owing to PEC conjugation might be responsible for the observed release increment. PEC conjugation with GO-Fe_3O_4 increases the hydrophilic character of the nanocarrier, due to the presence of oxygen containing groups (–COOH and –OH) on the PEC. At pH values greater than that of pKa's (~3.5 to 4.0) of PEC, the carboxylic acid groups of the PEC will be ionized resulting in electrostatic repulsion between the PEC chains [38]. This phenomenon facilitates water uptake by the nanocarrier causing swelling of the drug carrier and activates further PAC release [39–41].

Moreover, the release at pH 5.5 was found to be greater than that of pH 7.4, indicating pH-responsive release. The differences in release profile of GO-Fe_3O_4-PAC and PEC-GO-Fe_3O_4-PAC between 5.5 and 7.4 pH mediums were analysed and found to be statistically significant ($p < .05$). The reason for the observed pH-dependency release could be due to protonation of PEC-GO-Fe_3O_4 functional groups at acidic medium, resulting into partial dissociation of the hydrogen bonding between the drug and the carrier [42,43]. On the other hand, the possibility of relatively stronger hydrogen bonding interactions between the nanocarrier and the drug at neutral and basic conditions could result into an ineffective PAC release [43,44]. This result is very important for tumour specific drug delivery systems, since the cellular environment of tumour tissues is acidic.

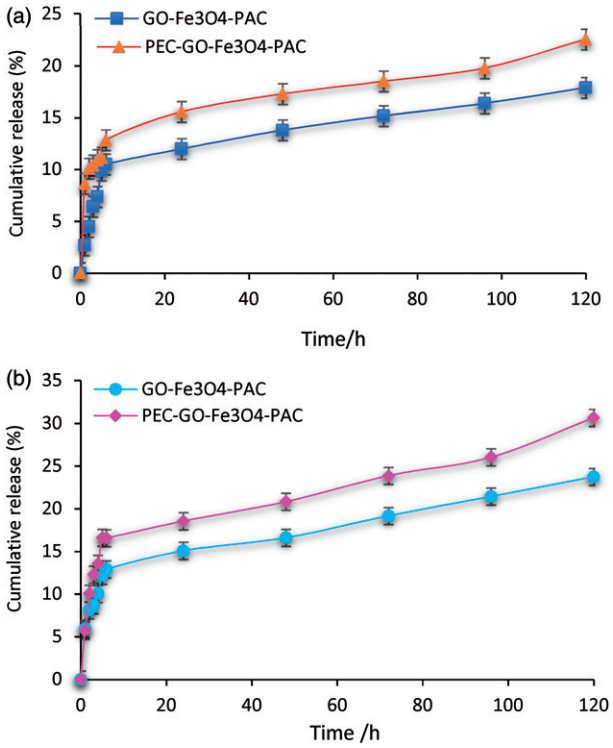

Figure 7. PAC release from GO-Fe_3O_4-PAC and PEC-GO-Fe_3O_4-PAC (a) at pH 7.4 and (b) at pH 5.5. Results were expressed as the mean ± SD of $n = 3$, $p < .05$.

Furthermore, drug release kinetics was evaluated following Korsmeyer–Peppas's model. According to this model, the release mechanism is determined by Equation (4).

$$\frac{M_t}{M_n} = kt^n \tag{4}$$

where M_t is the mass of PAC released at time t, M_n is the total mass of PAC loaded, k is the releasing rate constant and n is an exponent. The value of n indicates the nature of release mechanism; $n < 0.45$ related to Fickian diffusion, $n > 0.89$ to zero-order (case II) transport, and $0.45 < n < 0.89$ to non-Fickian or anomalous diffusion [45]. Table 2 presents n values for GO-Fe_3O_4-PAC and PEC-GO-Fe_3O_4-PAC at pH 7.4

and 5.5. As the table illustrated, the value of n was found to be less than 0.45 for both nanocarriers at pH 5.5 and 7.4. This n value showed that the release mechanism of PAC follows Fickian diffusion; that means, PAC release from both GO-Fe_3O_4-PAC and PEC-GO-Fe_3O_4-PAC nanocarriers is mainly governed by the drug diffusion [46].

Cytotoxicity study

To assess the biocompatibility of the synthesized GO-Fe_3O_4 and PEC-GO-Fe_3O_4 nanocarriers, MTT test was done using L-929 fibroblast as a normal cell. Figure 8 presents the relative cell viability of L-929 cell treated with GO-Fe_3O_4 and PEC-GO-Fe_3O_4. As it can be seen from the figure, the cell viability of both GO-Fe_3O_4 and PEC-GO-Fe_3O_4 nanocarriers is high (>75%) for all concentrations, indicating biocompatibility of the nanocarriers. However, PEC-GO-Fe_3O_4 showed relatively larger cell viability than that of GO-Fe_3O_4. From the result, it can be concluded that the conjugation of PEC with GO-Fe_3O_4 enhanced the biocompatibility of the nanocarrier.

On the other hand, the anti-tumour activities of GO-Fe_3O_4, PAC and loaded GO-Fe_3O_4 and PEC-GO-Fe_3O_4 nanocarriers on MCF-7 cancer cell were investigated. Figure 9 presents the relative cell viability of MCF-7 cancer cell treated with GO-Fe_3O_4, PAC and PAC loaded GO-Fe_3O_4 and PEC-GO-Fe_3O_4. The graph showed the relative cell viability of GO-Fe_3O_4 to be very high (>80%) at all concentrations due to its non-cytotoxic nature. However, PAC, GO-Fe_3O_4-PAC and PEC-GO-Fe_3O_4-PAC revealed a significant inhibition of MCF-7 cancer cell growth. Relative cell viability was observed to be less than 25% for pure PAC and PAC loaded carriers, at all concentrations greater than 250 ng mL^{-1}. When the concentration of PAC was lowered to 25 ng mL^{-1}, the cell viability increased to 31%, demonstrating a low concentration of PAC ($\leq$25 ng mL^{-1}) could inhibit the growth of cancer cells. On the other hand, at concentration, greater than 500 ng mL^{-1}, the toxicity of pure PAC, PAC loaded GO-Fe_3O_4 and PEC-GO-Fe_3O_4 is nearly similar, while, at concentration $\leq$250 ng mL^{-1}, the toxicity of PAC is observed relatively higher than that of PAC loaded nanocarriers.

Table 2. Release exponent (*n*), calculated from paclitaxel release profile using Korsmeyer–Peppas model.

Nanocarrier	pH of medium	Release exponent (*n*)	Regression (*r*)
GO-Fe_3O_4-PAC	5.5	0.25	0.9747
	7.4	0.32	0.9251
PEC-GO-Fe_3O_4-PAC	5.5	0.26	0.9309
	7.4	0.19	0.9929

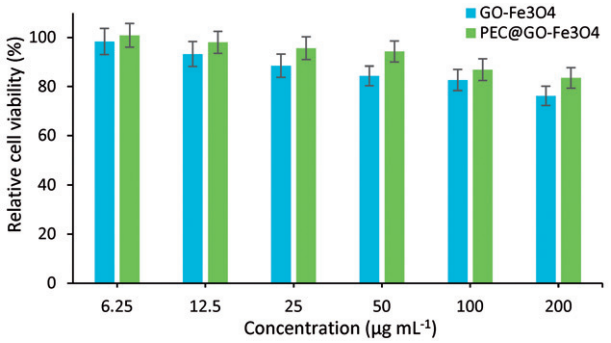

Figure 8. Relative cell viability of GO-Fe_3O_4 and PEC-GO-Fe_3O_4 treated with L-929 fibroblast normal cell. Data were revealed as the means ± SD ($n = 3$).

Conclusions

We have prepared a novel multi-functional magnetic GO based nanocarrier; that is non-toxic, more stable, and with superior drug loading and release performance. PEC as an ideal natural polymer, having high biocompatibility and non-toxic nature, was used to functionalize GO-Fe_3O_4. The prepared hybrid nanocarrier was analysed and interesting results were recorded. Cytotoxicity assay has shown GO-Fe_3O_4 and PEC-GO-Fe_3O_4 are biocompatible with more than 80% relative cell viability. Besides, the conjugation of PEC enhanced the biocompatibility of GO-Fe_3O_4. Drug loading and release assessment indicated the synthesized nanocarrier has great drug loading performance with pH-responsive release. At endosomal cancer cell medium, the release was found more than normal physiological environments, signifying the importance of the hybrid carrier for tumour targeted delivery

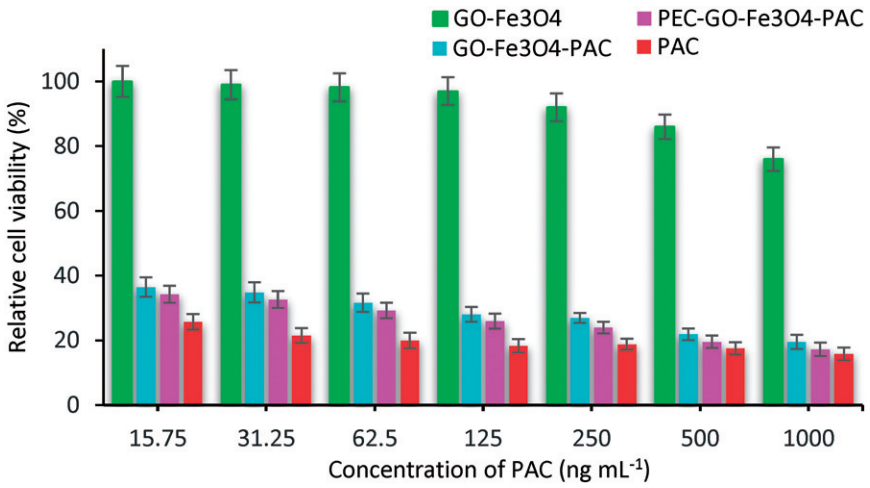

Figure 9. Relative cell viability of GO-Fe_3O_4-PAC and PEC-GO-Fe_3O_4-PAC treated with MCF-7 cancer cell. The points were expressed as mean ± SD of ($n = 3$).

systems. Moreover, surface morphology investigations and thermal analysis demonstrated the functionalization of GO-Fe_3O_4 with PEC has improved the colloidal and thermal stability of the GO-Fe_3O_4. In the light of these findings, the prepared multi-functional magnetic nanocarrier is expected to play a significant role in future drug carrier formulations for cancer treatment.

Disclosure statement

The authors report no conflicts of interest.

Funding

The authors thankfully acknowledge the fund support given by Kırıkkale University, under BAP project reference number 2017/055, 2017.

References

[1] Qin XC, Guo ZY, Liu ZM, et al. Folic acid-conjugated graphene oxide for cancer targeted chemo-photothermal therapy. J Photochem Photobiol B: Biol. 2013;120:156–162.
[2] Wang C, Ravi S, Garapati US, et al. Multifunctional chitosan magnetic-graphene (CMG) nanoparticles: a theranostic platform for tumor-targeted co-delivery of drugs, genes and MRI contrast agents. J Mater Chem B. 2013;1:4396–4405.
[3] Chuanyu S, Yu W. Synthesis and characterization of graphene oxide composite with Fe_3O_4. Mater Sci-Poland. 2015;33:11–13.
[4] Zhou T, Zhou X, Xing D. Controlled release of doxorubicin from graphene oxide based charge-reversal nanocarrier. Biomaterials. 2014;35: 4185–4194.
[5] Kavitha T, Kang I-K, Park S-Y. Poly (N-vinyl caprolactam) grown on nanographene oxide as an effective nanocargo for drug delivery. Colloids Surf B: Biointerfaces. 2014;115:37–45.
[6] Kavitha T, Kang IK, Park SY. Poly(acrylic acid)-grafted graphene oxide as an intracellular protein carrier. Langmuir. 2014;30: 402–409.
[7] Gao Y, Zou X, Zhao JX, et al. Graphene oxide-based magnetic fluorescent hybrids for drug delivery and cellular imaging. Colloids Surf B Biointerfaces. 2013;112:128–133.
[8] Wang Z, Zhou C, Xia J, et al. Fabrication and characterization of a triple functionalization of graphene oxide with Fe_3O_4, folic acid and doxorubicin as dual-targeted drug nanocarrier. Colloids Surf B Biointerfaces. 2013;106:60–65.
[9] Shan Y, Xu X, Chen K, Gao L. Preparation and characterization of magnetic graphene oxide. AMR. 2013;774:532–535.
[10] Yang X, Chen Y, Yuan R, et al. Folate-encoded and Fe_3O_4-loaded polymeric micelles for dual targeting of cancer cells. Polymer. 2008; 49:3477–3485.
[11] Kundu A, Nandi S, Das P, et al. Fluorescent graphene oxide via polymer grafting: an efficient nanocarrier for both hydrophilic and hydrophobic drugs. ACS Appl Mater Interfaces. 2015;7: 3512–3523.
[12] Lei H, Xie M, Zhao Y, et al. Chitosan/sodium alginate modificated graphene oxide-based nanocarrier as a carrier for drug delivery. Ceram Int. 2016;42:17798–17805.
[13] Pan Y, Bao H, Sahoo NG, et al. Water-soluble poly(n-isopropylacrylamide)-graphene sheets synthesized via click chemistry for drug delivery. Adv Funct Mater. 2011;21:2754–2763.
[14] Liu Z, Robinson JT, Sun X, et al. PEGylated nanographene oxide for delivery of water-insoluble cancer drugs. J Am Chem Soc. 2008;130: 10876–10877.
[15] An J, Gou Y, Yang C, et al. Synthesis of a biocompatible gelatin functionalized graphene nanosheets and its application for drug delivery. Mater Sci Eng C Mater Biol Appl. 2013;33: 2827–2837.
[16] Mianehrow H, Moghadam MHM, Sharif F, et al. Graphene – oxide stabilization in electrolyte solutions using hydroxyethyl cellulose for drug delivery application. Int J Pharm. 2015;484: 276–282.
[17] Ngenefeme F-TJ, Eko NJ, Mbom YD, et al. A one pot green synthesis and characterisation of iron oxide-pectin hybrid nanocomposite. Open J Compos Mater. 2013;3:30–37.
[18] Thi Tran TT, Thi Le HN, Van Tran H, et al. *Tithonia diversifolia* pectin – reduced graphene oxide and its cytotoxic activity. Mater Lett. 2016;183:127–130.
[19] Mishra RK, Datt M, Banthia AK. Synthesis and characterization of pectin/PVP hydrogel membranes for drug delivery system. AAPS PharmSciTech. 2008;9:395–403.
[20] Munarin F, Giuliano L, Bozzini S, et al. Mineral phase deposition on pectin microspheres. Mater Sci Eng C. 2010;30:491–496.
[21] Munarin F, Guerreiro SG, Grellier MA, et al. Pectin-based injectable biomaterials for bone tissue engineering. Biomacromolecules. 2011;12:568–577.
[22] Munarin F, Petrini P, Tanzi MC, et al. Biofunctional chemically modified pectin for cell delivery. Soft Matter. 2012;8: 4731–4739.
[23] Zahran MK, Ahmed HB, El-Rafie MH. Facile size-regulated synthesis of silver nanoparticles using pectin. Carbohydr Polym. 2014;111: 971–978.
[24] Kilicay E, Erdal E, Hazer B, et al. Antisense oligonucleotide delivery to cancer cell lines for the treatment of different cancer types. Artif Cells Nanomed Biotechnol. 2016;44:1938–1948.
[25] Mirahmadi F, Tafazzoli-Shadpour M, Shokrgozar MA, et al. Enhanced mechanical properties of thermosensitive chitosan hydrogel by silk fibers for cartilage tissue engineering. Mater Sci Eng C Mater Biol Appl. 2013;33:4786–4794.
[26] Xie G, Xi P, Liu H, et al. A facile chemical method to produce superparamagnetic graphene oxide-Fe_3O_4 hybrid composite and its application in the removal of dyes from aqueous solution. J Mater Chem. 2012;22:1033–1039.
[27] Wang G, Chen G, Wei Z, et al. Multifunctional Fe_3O_4/graphene oxide nanocomposites for magnetic resonance imaging and drug delivery. Mater Chem Phys. 2013;141:997–1004.
[28] Kassaee MZ, Motamedi E, Majdi M. Magnetic Fe_3O_4-graphene oxide/polystyrene: fabrication and characterization of a promising nanocomposite. Chem Eng J. 2011;172:540–549.
[29] Yu L, Wu H, Wu B. Magnetic Fe_3O_4-reduced graphene oxide nanocomposites-based electrochemical biosensing. Nano-Micro Lett. 2014; 6:258–267.
[30] Salem NM, Awwad AM. A novel approach for synthesis magnetite nanoparticles at ambient temperature. Nanosci Nanotechnol. 2013;3:35–39.
[31] Kadam AA, Jang J, Lee DS. Facile synthesis of pectin-stabilized magnetic graphene oxide prussian blue nanocomposites for selective cesium removal from aqueous solution. Bioresour Technol. 2016;216:391–398.
[32] Ebrahimi E, Akbarzadeh A, Abbasi E, et al. Novel drug delivery system based on doxorubicin-encapsulated magnetic nanoparticles modified with PLGA-PEG_{1000} copolymer. Artif Cells Nanomed Biotechnol. 2016;44:290–297.
[33] Ebrahimi E, Khandaghi AA, Valipour F, et al. *In vitro* study and characterization of doxorubicin-loaded magnetic nanoparticles modified with biodegradable copolymers. Artif Cells Nanomed Biotechnol. 2016;44:550–558.
[34] More MP, Patil MD, Pandey AP, et al. Fabrication and characterization of graphene-based hybrid nanocomposite: assessment of antibacterial potential and biomedical application. Artif Cells Nanomed Biotechnol. 2017;45:1496–1508.
[35] Swain AK, Pradhan L, Bahadur D. Polymer stabilized Fe_3O_4-graphene as an amphiphilic drug carrier for thermo-chemotherapy of cancer. ACS Appl Mater Interfaces. 2015;7:8013–8022.
[36] Rana VK, Choi MC, Kong JY, et al. Synthesis and drug-delivery behavior of chitosan-functionalized graphene oxide hybrid nanosheets. Macromol Mater Eng. 2011;296:131–140.

[37] Muthoosamy K, Bai RG, Manickam S. Graphene and graphene oxide as a docking station for modern drug delivery system. Curr Drug Deliv. 2014;11:701–718.

[38] Jung J, Arnold RD, Wicker L. Pectin and charge modified pectin hydrogel beads as a colon-targeted drug delivery carrier. Colloids Surf B Biointerfaces. 2013;104:116–121.

[39] Rasoulzadeh M, Namazi H. Carboxymethyl cellulose/graphene oxide bio-nanocomposite hydrogel beads as anticancer drug carrier agent. Carbohydr Polym. 2017;168:320–326.

[40] Amoli-diva M, Pourghazi K. Poly(methacrylic acid-co-acrylic acid)-grafted polyvinylpyrrolidone coated magnetic nanoparticles as a pH-responsive magnetic nano-carrier for controlled delivery of antibiotics. Nanomed J. 2017;4:25–36.

[41] Modaresifar K, Hadjizadeh A, Niknejad H. Design and fabrication of GelMA/chitosan nanoparticles composite hydrogel for angiogenic growth factor delivery. Artif Cells Nanomed Biotechnol. 2017 [Oct 24];[1–10]. doi: 10.1080/21691401.2017.1392970

[42] Khoee S, Bafkary R, Fayyazi F. DOX delivery based on chitosan-capped graphene oxide-mesoporous silica nanohybride as pH-responsive nanocarriers. J Sol–Gel Sci Technol. 2017;81:493–504.

[43] Fan X, Jiao G, Zhao W, et al. Magnetic Fe_3O_4-graphene composites as targeted drug nanocarriers for pH-activated release. Nanoscale. 2013; 5:1143–1152.

[44] Zhang L, Xia J, Zhao Q, et al. Functional graphene oxide as a nanocarrier for controlled loading and targeted delivery of mixed anticancer drugs. Small. 2010;6:537–544.

[45] Luo H, Ao H, Li G, et al. Bacterial cellulose/graphene oxide nanocomposite as a novel drug delivery system. Curr Appl Phys. 2017;17(2):249–254.

[46] Isıklan N, Küçükbalcı G. Microwave-induced synthesis of alginate-graft-poly(N-isopropylacrylamide) and drug release properties of dual pH- and temperature-responsive beads. Eur J Pharm Biopharm. 2012;82:316–331.